23rd ABCM International Congress of Mechanical Engineering
December 6-11, 2015, Rio de Janeiro, RJ, Brazil

ITERATIVE INVERSE KINEMATICS OF AN UNDERACTUATED 5 D.O.F. SERVICE ROBOT FOR REPAIRING HYDRAULIC TURBINE BLADES

José Maurício S. T. Motta
Carlos H. Llanos Quintero
Renato Coral Sampaio
Guilherme Caribé de Carvalho
Sadek C. Absi Alfaro
Universidade de Brasilia, Dept. Mechanical Eng., Asa Norte, Brasília-DF, Brazil
70910-900
jmmotta@unb.br; llanos@unb.br; renatocoral@gmail.com

Abstract. *This paper presents and discusses partial results of an ongoing R&D project aiming to design and build a fully automated prototype of a specialized robotic welding system for repairing hydraulic turbine surfaces eroded by cavitation pitting and/or cracks produced by cyclic loading. The system has an embedded vision sensor built to acquire range images by laser scanning over the blade surface and produce 3D models to locate the damaged spots to be registered in a 3D coordinate system into the robot controller, enabling the robot to repair the flaws automatically by welding in layers. The paper is focused on the robot kinematic model and proposes an iterative algorithm to solve the inverse kinematics problem of the underactuated robot with 5 degrees-of-freedom. The iterative algorithm makes use of data collected from a vision sensor to ensure that the welding gun axis is perpendicular to the blade surface. Experimental results show that the iterative algorithm to perform the inverse kinematics proved to be very efficient.*

Keywords: *Iterative Inverse Kinematics, Turbine Blade Repairing, Automated Welding Robots, Underactuated Robots.*

1. INTRODUCTION

Blade surfaces of hydraulic turbines eroded by cavitation pitting or damaged by fatigue cracks are repaired by welding in layers with electric arc as a standard process (Parma, 1997; Ecober, *et al.*, 2006; Hammit, 1979). The repairing process is carried out manually after visual inspection of the blade surface, requiring a turbine halt. This is an undesirable human labor condition, with harsh air temperatures and air humidity for long periods of time. This article is concerned to a robot that was designed to improve the quality of the cavitation and/or fatigue damage repairing process, achieving a better surface profile after repairing, reducing welding defect rates and improving its consistency, reducing material consumption, time to repair and overall costs.

A robot designed to perform this type of task must have the capacity to weld with a large variation of torch orientation angles, it has to be small, light, accurate and resilient to loads from various directions. It has also to be resilient to deflections and have to be fixed at many different positions. Some of these characteristic performances are antagonistic, which means the achievement of one goal produces performance reduction in others. However, although some service robots have already been constructed for turbine blade repairing (Hazel, *et al.*, 2012; Chen, *et al.*, 2008; Xiang, *et al.*, 2010), this robot shows improvements to the previous, since it was designed to be completely automated, with little human action when in operation. In addition, this robot can operate inside large turbines, with 8 m in diameter and at least 500 mm in between blades (Motta, *et al.*, 2010a; Motta, *et al.*, 2010b; Motta, *et al.*, 2014).

It is widely accepted that manipulators designed for dexterity and for the easiness of kinematic models must have 6 degrees-of-freedom (d.o.f.) or more. Nevertheless, this robot was designed to have its dexterity limited to 5 d.o.f. for light weight, small size and for good portability. This solution is accepted considering that the welding torch nozzle is cylindrical, so one of the rotation angles is not needed for the torch tip orientation within the 3D space.

This article aims at presenting details of the robot kinematic model and an iterative algorithm developed for the robot inverse kinematics with the restriction of only 5 d.o.f.. The algorithm is input with data collected from a 3D vision sensor that sends structured data from regions of the blade surface to be repaired, in such a way that the welding gun axis is perpendicular to the surface to be welded. Some other proposals to iteratively calculate the inverse kinematics for 5 d.o.f. robots have already been published by other researchers, but with different robot topologies and more complicate strategies (Su, et al., 2005; Park, et al., 2012; Liu, et al., 2012).

2. THE ROBOT PROTOTYPE

The robot constructed weights 30kg, has a spherical topology and a 2.0m outer diameter workspace with 30 x 25 x 60-100cm in dimensions without the welding torch. Figure 1 shows the constructed system. (Motta, *et al*., 2010a)

The robotic system has a pan-tilt wrist, three electric stepper motors, rotary and linear actuators. The robot arm carries an embedded 3D vision sensor for range image acquisition in the form of point clouds and for modeling 3D structured surface maps with special modeling and image registering algorithms. The 3D maps are included with welding trajectories in 3D coordinates automatically, according to the welding strategy to weld the surface blade region. The measurement system software is implemented in a mini-PC embedded on the system. The robot and welding controller systems are designed and built on a reconfigurable architecture based on FPGA (Field Programmable Gate Arrays). The welding process type used is the GMAW (Gas Metal Arc Welding) with a pulsed arc welding machine and tubular metal cored electrodes. (Motta, *et al.*, 2014). The robot has an embedded integrated control system for managing several tasks to be carried out automatically. The control system was designed to manage the robot actions such as (a) environment recognition, (b) calculation of volumes and location to be filled with weld beads, (c) slicing the volumes by using welding strategies to weld in layers, (d) calculating trajectories for the welding torch and (e) managing the robot motion according to the welding needs.

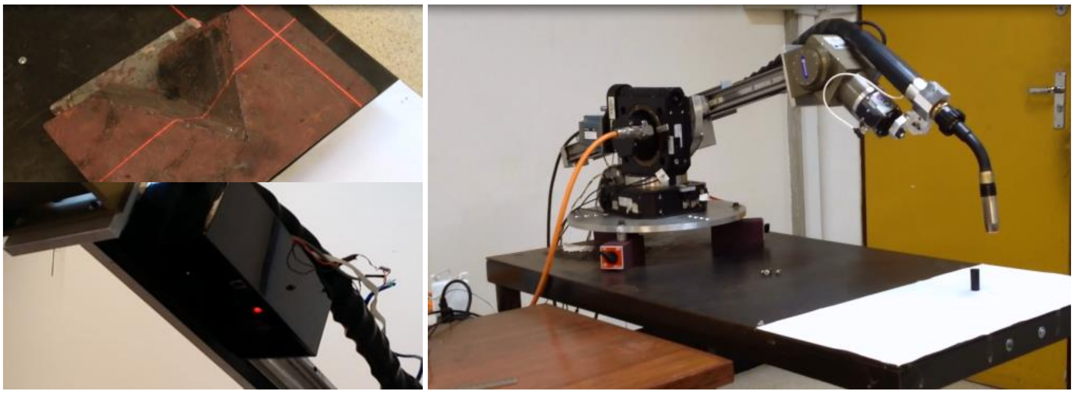

Figure 1. Robot prototype

3. KINEMATIC SYSTEM

3.1 Assignment of Joint Coordinate Frames

Joint coordinate systems have been assigned to the robot kinematic model in such a way that the **Zn** axes point towards the joint axis of motion and that the vectors **Xn** are all parallel when the robot is in its zero position. The **Yn** axes are orthogonal to the formers, creating an orthonormal systems of axes. The origins of the coordinate frames are located using a minimum number of link parameters (Motta, 2006).

A coordinate frame is attached to the end-effector such that the z-axis of the frame has the same direction of the z-axis of the frame placed at the last joint (*n-1*). For this robot, it is also necessary to have a separate transformation for this last frame, which is fixed at the welding torch tip, to ensure that its z-axis is parallel to the axis of symmetry of the torch nozzle, ensuring a proper control of the welding torch orientation.

Link length parameters are represented in the model with indexes for joints and direction. The *pki* link length is the distance between the origins of the coordinate frames *i-1* and *i*, such as *k* is the axis of the coordinate frame *i-1* that is parallel to the length direction. Figure 2a shows this convention applied to the robot with all coordinate frames, geometric parameters and link variables.

3.2 Forward Kinematic Model

Homogeneous transformation matrices that relate coordinate frames from the base (b) to the torch/tool (t) frames can be derived as:

$$ {}_t^bT = {}_0^bT * {}_1^0T * {}_2^1T * {}_3^2T * {}_4^3T * {}_5^4T * {}_t^5T = \begin{bmatrix} n_x & o_x & a_x & p_x \\ n_y & o_y & a_y & p_y \\ n_z & o_z & a_z & p_z \\ 0 & 0 & 0 & 1 \end{bmatrix}, \qquad (1) $$

where ${}_{i+1}^{i}T$ is the homogeneous transformation between two successive joint coordinate frames. The welding gun is attached to link 4 and its geometric parameters can be seen in Fig. 2b. The transformations shown in Eq. (1) can be calculated from the Denavit-Hartemberg (D-H) notation as:

$$ {}^{i-1}_{i}T = Rz(\theta) * Tz(d) * Tx(l) * Rx(\alpha) = \begin{bmatrix} \cos(\theta) & -(\cos(\alpha) * \sin(\theta)) & \sin(\alpha) * \sin(\theta) & l * \cos(\theta) \\ \sin(\theta) & \cos(\alpha) * \cos(\theta) & -(\cos(\alpha) * \sin(\theta)) & l * \sin(\theta) \\ 0 & \sin(\alpha) & \cos(\alpha) & d \\ 1 & 0 & 0 & 1 \end{bmatrix}, \quad (2) $$

where θ and α are rotation parameters, d and l are translation parameters. The last homogeneous transformation rotates the coordinate system 5 around the **y5** vector, according to the cylindrical shape of the torch nozzle. This transformation is necessary for the **Zt** axis to be aligned with the torch axis of symmetry, such as

$$ {}^{5}_{t}T = \begin{bmatrix} \cos(\beta) & 0 & \sin(\beta) & 0 \\ 0 & 1 & 0 & 0 \\ -\sin(\beta) & 0 & \cos(\beta) & 0 \\ 1 & 0 & 0 & 1 \end{bmatrix} \quad (3) $$

The entries of the general manipulator transformation, ${}^{0}_{5}T$, according to Eq. (1), excluding the rotation of the torch tip coordinate frame by the angle β, can be seen in Table 1, as the robot forward kinematic equations. Equations (4a-4*l*) are formulated by the application of Eq. (2) to each of the successive robot joint frames by using the geometric parameters shown in Fig. 2a and Fig. 2b.

Table 1. Forward kinematic equations according to Eq.(1).

$nx = -\sin(\theta1).\sin(\theta5) + \cos(\theta5).\cos(\theta1).\cos(\theta2+\theta4)$	(4a)
$ox = -\sin(\theta1).\cos(\theta5) - \sin(\theta5).\cos(\theta1).\cos(\theta2+\theta4)$	(4b)
$ax = \cos(\theta1).\sin(\theta2+\theta4)$	(4c)
$px = \mathrm{pz3}.\cos(\theta1).\sin(\theta2) + px2.\sin(\theta1).\sin(\theta2) - pz2.\sin(\theta1) + pz5.\cos(\theta1).\sin(\theta2+\theta4) + px5.[\cos(\theta1).\cos(\theta2+\theta4)] - \sin(\theta1).\sin(\theta5)]$	(4d)
$ny = \cos(\theta1).\sin(\theta5) + \cos(\theta5).\sin(\theta1).\cos(\theta2+\theta4)$	(4e)
$oy = \cos(\theta1).\cos(\theta5) - \sin(\theta5).\sin(\theta1).\cos(\theta2+\theta4)$	(4f)
$ay = \sin(\theta1).\sin(\theta2+\theta4)$	(4g)
$py = pz3.\sin(\theta1).\sin(\theta2) - \mathrm{px2}.\sin(\theta1).\cos(\theta1) + \mathrm{pz2}.\cos(\theta1) + \mathrm{pz5}.\sin(\theta1).\sin(\theta2+\theta4) + \mathrm{px5}.[\cos(\theta1).\sin(\theta5) + \cos(\theta5).\sin(\theta1).\cos(\theta2+\theta4)]$	(4h)
$nz = -\sin(\theta2+\theta4).\cos(\theta5)$	(4i)
$oz = \sin(\theta2+\theta4).\sin(\theta5)$	(4j)
$az = \cos(\theta2+\theta4)$	(4k)
$pz = \mathrm{pz1} + \mathrm{pz5}.\cos(\theta2+\theta4) + pz3.\cos(\theta2) + px2.\sin(\theta2) - px5.\sin(\theta2+\theta4).\cos(\theta5)$	(4*l*)

3.3. Inverse Kinematic Model

During the robot motion, the vision sensor provides the normal vector to the surface to be welded, **Z**, calculated at the point to be welded, related to the robot base coordinate frame. Considering the **Zt** vector as parallel to the nozzle axis of symmetry and pointing outwards, as it is shown in Fig. 2a and Fig. 2b, it is needed to establish the triplet **Ωt = [Xt, Yt, Zt]** on the welding torch tip such that the torch reaches the desired position coordinate point, **P=[Px, Py, Pz]**, with the torch tip **Zt** axis oriented in the direction of the surface normal vector, **Z**.

According to the kinematic model shown in Fig. 2a, with θ5 at its zero position, the vectors **Xt** and **Zt** belong to a plane π, shown in Fig. 3a, passing through the torch tip and links 4 and 3.

It is assumed that **Z** is a unit vector. Thus, **Zt = -Z**, and according to Fig. 3, one can calculate the vector **V**, belonging to the plane π, as:

V = [Px + d2. sen(α) , Py - d2. cos(α) , Pz], (6)

in which α = atan(**Py/Px**) – asin (d2/||**P**||).

The triplet **Ωt** = **[Xt, Yt, Zt]** can be calculated from

Yt =(-Z) x (-V) ; **Xt = (-Z) X (-Yt)** ; **Zt = -Z** (5)

The vectors **Xt** and **Yt** are therefore calculated assuming that **Xt** belongs to the plane π, i.e. θ5 = 0. However, for a solution for the triplet **Ωt** for any non-zero value of θ5, **Xt** and **Yt** calculated from Eq. (6) is close to the solution and will be used as initial values in a simple iterative method to be described later in this article.

A general orientation transformation Hp_0 can be formulated as

$$Hp_0 = \begin{bmatrix} Xt_x & Yt_x & Zt_x & P_x \\ Xt_y & Yt_y & Zt_y & P_y \\ Xt_z & Yt_z & Zt_z & P_z \\ 0 & 0 & 0 & 1 \end{bmatrix} = \begin{bmatrix} \boldsymbol{R} & \boldsymbol{P} \\ \boldsymbol{0} & 1 \end{bmatrix}, \tag{7}$$

whose the first three columns determine the components of the vectors **Xt, Yt, Zt** in the robot base coordinate frame respectively.

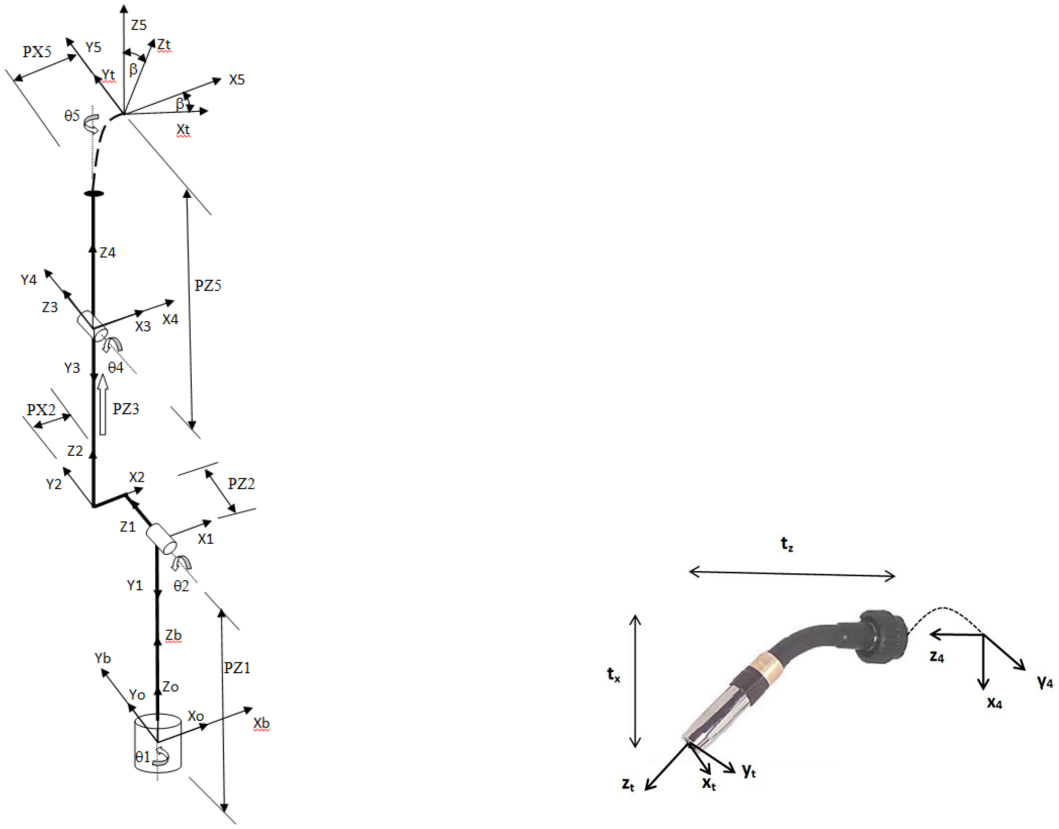

(a) (b)

Figure 2. (a) Robot at zero position with joint coordinate systems and link variables; (b) Welding torch coordinate frame (x_t, y_t, z_t) and related geometric parameters (t_x , t_z)

The robot inverse kinematics provides all the joint values in Eqs. (4a) to (4*l*), shown in Table 1. However, Eq. (1) is not equal to Eq. (7), except in the case of θ5 = 0.

In the case of this robot, the robot inverse kinematics equations can be found geometrically. To achieve that the torch coordinate frame should be rotated around **Yt** by an angle -β, such that the **Zt** axis gets back to its orientation to be collinear to the **Z5** vector. The vector system **(X5, Y5, Z5)** at the torch tip becomes parallel to the vector system **(X4, Y4, Z4)** of the flange. Therefore,

$${}^{0}_{5}T = Hp_0 * {}^{5}_{t}T^{-1} = Hp_0 * {}^{t}_{5}T \tag{8}$$

The transformation ${}^{t}_{5}T$ yields an elementary rotation around the **Yt** axis. Equations (4i) and (4j) can be manipulated algebraically to make θ5 explicit. There are two solutions for θ5:

$$\theta 5_1 = \tan^{-1}\left(\frac{Yt_z}{Xt_z}\right) \quad ; \quad \theta 5_2 = \tan^{-1}\left(-\frac{Yt_z}{Xt_z}\right) \tag{9}$$

If the component of the product **(V)** x **(Z)** in the **Zb** direction is positive the solution chosen for θ5 is negative, if it is negative the solution chosen is positive.

From Eqs. (4c) and (4g), and by using the orthonormality of the rotation matrix, **R**, in Eq.(7), then

$$n_z{}^2 + o_z{}^2 + a_z{}^2 = 1 \quad \text{and} \quad a_x{}^2 + a_y{}^2 + a_z{}^2 = 1 \quad , \tag{10}$$

and θ1 can be made explicit as

$$\theta 1_1 = -2 * \tan^{-1}\left[\frac{\sqrt{2*(n_z{}^2+o_z{}^2)-(a_x{}^2+a_y{}^2)}-\sqrt{n_z{}^2+o_z{}^2}}{a_x+a_y+\sqrt{n_z{}^2+o_z{}^2}}\right] \tag{11a}$$

$$\theta 1_2 = \ 2 * \tan^{-1}\left[\frac{\sqrt{2*(n_z{}^2+o_z{}^2)-(a_x{}^2+a_y{}^2)}-\sqrt{n_z{}^2+o_z{}^2}}{a_x+a_y+\sqrt{n_z{}^2+o_z{}^2}}\right], \tag{11b}$$

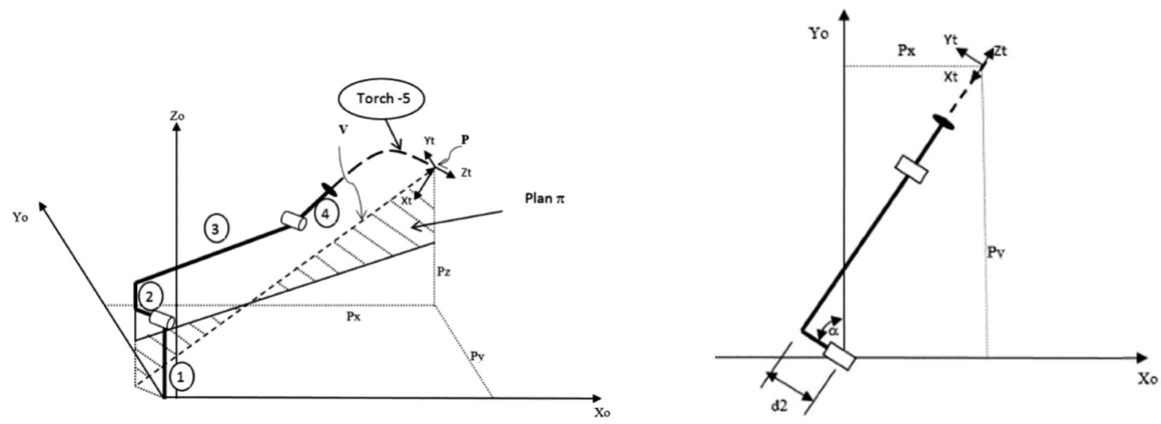

(a) (b)

Figure 3. The robot position with the torch coordinate system oriented when the angle θ5 = 0.

The equations above present a singularity for $a_z = \mp 1$, i.e. $n_z = o_z = a_x = a_y = 0$, where the flange **Z4** axis is collinear with the robot base **Zb** axis. This particular robot configuration can be easily avoided.

The correct solution for θ1 must be chosen from the sign of the *z* components of the normal vector to the plane π formed by the vectors **P** and **Z**.

Closed equations for the joint variables θ4, θ2 and pz3 cannot be easily formulated from the robot general transformation matrix, but they can be expressed using geometry. From Eq. (8) and Eq. (2) one can determine the position of the origin of the coordinate frame 4, **(Px4, Py4, Pz4)**, through the equation:

$${}^0_4T = {}^0_5T * {}^4_5T^{-1} = {}^0_5T * {}^5_4T \ , \tag{12}$$

where the origin position is described from the entries of the fourth column of the ${}^0_4T$ transformation.

From Figs. 3a and 3b, pz3 can be obtained as:

$$pz3 = \sqrt{(l^2 + (Pz4 - pz1)^2 - px2^2)} \tag{13}$$

in which $l = \sqrt{(Px4^2 + Py4^2 - pz2^2)}$

The variable θ2 can be formulated from

$$\theta 2 = \pi - \sin^{-1}\left(\frac{pz3}{\sqrt{(l^2+(Pz4-pz1)^2)}}\right) - \sin^{-1}\left(\frac{Pz4-pz1}{\sqrt{l^2+(Pz4-pz1)^2}}\right) \tag{14}$$

The variable θ4 can be obtained from

$$\theta 4 = \cos^{-1}(a_z) - \theta 2 \tag{15}$$

It is clear from the equations above that θ5, θ1 and (θ4+θ2) only carry information from the torch orientation, while pz3, θ2 and θ4 define its position.

4. INVERSE KINEMATICS SOLUTION

Equations (9), (11), (13), (14) and (15) give a closed solution for the robot inverse kinematics, once proper values for the welding torch orientation vectors, **Xt** and **Yt**, are available. Despite of that, a robot with 5 d.o.f. cannot locate its end-effector/tool at every pose within its workspace, which means that one of the three orientation angles cannot be chosen freely with a 2 d.o.f pan-tilt wrist. Equation (1) cannot be solved for every robot's pose in Eq. (6). In other words, since a torch orientation vector, **Zt**, is chosen the first two columns of the rotation transformation matrix, **R**, in Eq. (7), cannot be determined in order to produce the inverse kinematics solution that will move the welding torch to the correct pose **P=(Px, Py, Pz)**.

One way to tackle this problem is to make use of an iterative method that varies **Xt** and **Yt** in Eq. (7) up till the solution of Eq. (1) converges to the correct pose with the desired **Zt**.

4.1 Algorithm Description

Once the welding nozzle has a cylindrical geometry, it can be assumed that the rotation around its axis of symmetry does not need to be specified (around **Zt**). In this way, the orientation angle of the orthonormal vectors, **Xt** and **Yt,** cannot be specified, but it can be found numerically as a function of the other components of the robot kinematic model. So, an initial value for ϕ (angle around **Zt**) can be specified as a function of the joint angles $\theta 5$ and $\theta 1$ (they depend only on the general orientation), which are independent of the torch position, **P**. The variables $\theta 2$, $\theta 4$ and pz3 depend on the torch orientation and also on its position.

The principle of the algorithm is based on the calculation of the relative angle, ϕ, between two 2D rotation matrices. An arbitrary reference angle is chosen as an initial value for the triplet **Ωt**, and the other angle is calculated from the equations of the inverse and forward kinematics so to calculate the relative angle between the two orientation angles. The algorithm starts with the choice of an initial value for the **Xt** and **Yt** vectors in Eq. (6), since **Zt** is provided by the vision sensor (vector normal to the surface). The second matrix can be calculated from the forward kinematics using the joint variable values obtained from the inverse kinematics (Eqs. (4)). So, orthonormal matrices can be formulated as

$$\begin{bmatrix} Xt_x & Yt_x \\ Xt_y & Yt_y \\ Xt_z & Yt_z \end{bmatrix} = \begin{bmatrix} n_x & o_x \\ n_y & o_y \\ n_z & o_z \end{bmatrix} * \begin{bmatrix} \cos \emptyset \\ \sin \emptyset \end{bmatrix} \tag{16}$$

Orthonormal matrices have a null scalar product between 2 columns/rows and the norms of the columns/rows are unitary. Then, it can be easily demonstrated that $Xt_x . o_x + Xt_y . o_y + Xt_z . o_z = \sin \emptyset$ and $Xt_x . n_x + Xt_y . n_y + Xt_z . n_z = \cos \emptyset$**.** So

$$\emptyset = \tan^{-1} \frac{Xt_x . o_x + Xt_y . o_y + Xt_z . o_z}{Xt_x . n_x + Xt_y . n_y + Xt_z . n_z} \ , \tag{17}$$

where ϕ is the relative rotation angle of the pair [X**t, Yt]** around the **Zt** axis calculated from the two matrices. The proposed algorithm can be established in the following steps:

1. The torch orientation, **Ωt = [Xt, Yt, Zt]**, is firstly supposed according to Eq. (6). The torch position vector, **P=[X, Y, Z]**, represented in the robot base coordinate frame is known and **Zt** is obtained from the vision sensor.
2. Equation (8) is used to rotate the triplet **Ωt** around **Yt**, aligning the torch tip coordinate frame with the coordinate system 5, $\mathbf{\Omega_5}$, linked to the robot flange. This keeps the system $\mathbf{\Psi_t}$ = **[P**, $\mathbf{\Omega_5}$**]** on the torch tip.
3. Equations (9-15) are used to determine the joint variable values, **[Θ]**, corresponding to the torch pose $\mathbf{\Psi_t}$.
4. Equations (4) are applied to calculate the forward kinematics, finding the robot position, **Pt**, with the joint coordinates, **[Θ]**, calculated in step 3.
5. The difference between the position specified, **P**, in step 1, and the position calculated in step 4, **Pt**, is found. This difference establishes a position error **ΔPt**. The difference between the torch orientation **Ωt** and the new orientation **Ωt'**, around **Zt**, is the angle ϕ, which can be calculated from Eq. (17). This difference shall be null with this proposed robot.

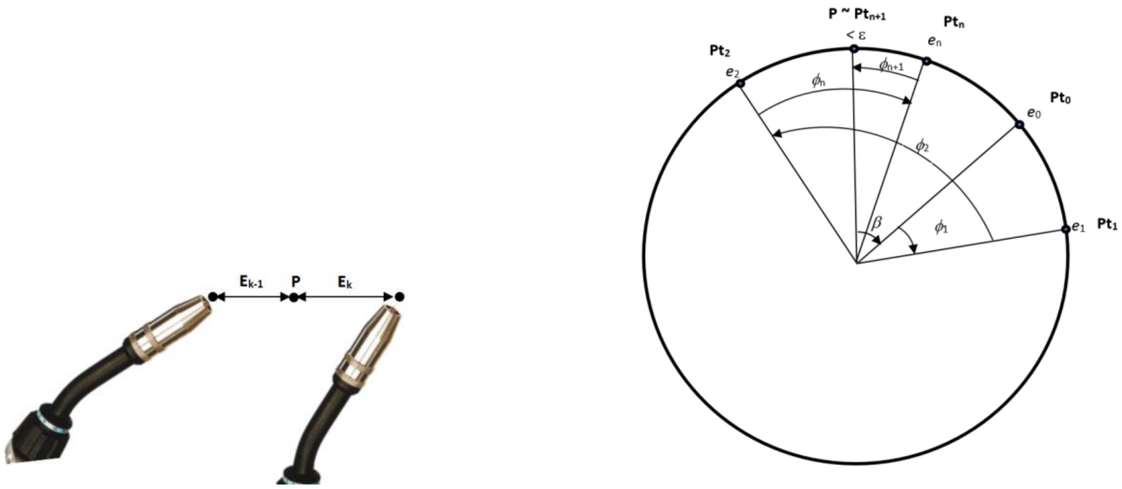

(a) (b)

Figure 4. (a) Positioning error of the welding torch in each iteration *k*. (b) Graphical demonstration of the rotation of **Xt** and **Yt** around the **Zt** axis by an angle ϕ, in successive iterations. For each position **Pt** attained, the error and the angle ϕ are shown. The value of ϕ is initially unknown (= β).

Once the vectors **P, Pt, ΔPt** and **Ωt** are available, a routine is applied to update the orientation triplet, **Ωt,** in such a way that the values of **ΔPt** are reduced to a minimum specified value, ε, upon which **Ωt** would provide the correct orientation of the torch. The rule for updating **Ωt** is to consider that the deviation of ϕ from its correct value is proportional to the Euclidean error, $e_k = |\mathbf{E_K}|$, in which $\mathbf{E_k} = \mathbf{\Delta Pt = P\text{-}Pt_k}$, between the torch tip position and its desired position, **P**, in each iteration *k*, as shown in Fig. 4a.

It is assumed that each value of ϕ_k in an iteration corresponds to a $\mathbf{E_k}$ position error. Fig. 4b represents, graphically, each value of ϕ_k in successive iterations until the solution. The proportional relationship between ϕ_κ and e_k can be established graphically as shown in Fig. 4b as:

$$\frac{\beta}{\beta+\phi_1} = \frac{e_0}{\mp e_1} \quad ==> \quad \frac{\phi_{k+1}}{\phi_{k+1}+\phi_k} = \frac{e_{k-1}}{\pm e_k} \quad ==> \quad \phi_{k+1} = \frac{e_{k-1}}{e_{k-1} - sign([E_{k-1}.E_k]e_k}\phi_k \tag{18}$$

Equation (18) provides a new rotation value ϕ_{k+1}, $\forall k : (1 \le k \le n)$, in each iteration *k*, until the error e_{n+1} between **P** and $\mathbf{Pt_{n+1}}$ is smaller than ε. The final value for ϕ, the angle γ, is measured between the orientation of the torch coordinate system proposed by Eq. (1) and the correct one. For this robot, as long as algorithm stops at the solution, Eq. (17) provides a value for γ that is numerically approximate to the solution for θ5.

4.2 Results of the Inverse Kinematics Algorithm

To verify the algorithm efficiency to find the inverse kinematic solution iteratively different robot poses were tested. All cases have demonstrated that the algorithm converges to the solution with at most four iterations. Input variables are the position of the surface point to be touched by the welding gun and the normal vector to the surface obtained from the vision sensor, both related to the robot base frame. The torch orientation have to coincide with normal vector furnished by the vision sensor. The robot link lengths were defined as in Table 2.

Table 2. Robot geometric parameters, such as in Fig. 2.

pz1 (mm)	pz2 (mm)	pz5 (mm)	px2 (mm)	px5 (mm)
275	105	480	32.3	15

One case of pose data input into the iterative algorithm was $P = [560 \quad 350 \quad 10]$ and $Z = [0.2 \quad -0.1 \quad 1]/1.0247$. Results showing the convergence of the joint values at each iteration are shown in Table 3. A chosen value for ε may be 0.2 mm, which interrupts the algorithm typically in the third iteration.

Table 3. Variable joint values and geometric parameters at each iteration of the algorithm.

Iteration	0	1	2	3

e(mm)	168.587	44.457	2.841	0.163
θ_1 (deg)	30.769	13.065	16.857	16.616
θ_2 (deg)	81.521	80.677	80.728	80.724
d_3 (mm)	378.131	416.652	405.843	406.86
θ_4 (deg)	61.362	64.660	64.155	64.190
θ_5 (deg)	15.053	11.357	12.254	12.202
ϕ (deg)	15.058	-3.142	0.189	-0.008

5. CONCLUSIONS

This article presented a robot constructed to repair the surface of hydraulic turbine blades eroded by cavitation or fatigue damage by welding in layers automatically using a 3D surface map acquired from a specialized vision sensor for managing the welding strategy. The vision sensor measures the surface normal vector at the point to be welded and this vector is used as input to an iterative algorithm to find the solution of the inverse kinematics of the under-actuated manipulator. The discussion is focused on the robot kinematic model and on details of the algorithm to perform the inverse kinematics iteratively. Experimental results show that the iterative algorithm is very efficient, converging to the solution in up to four iterations.

6. ACKNOWLEDGMENTS

This work had been supported by ELETRONORTE (Electrical Power Plants of the North of Brazil) and FINATEC (Foundation for Scientific and Technological Enterprises).

5. REFERENCES

Chen, Q., Sim, Z., Zhang, W., and Gui, Z., 2008. “A Robot for Welding Repair of Hydraulic Turbine Blade”. In *Conference on Robotics, Automation and Mechatronics*, Chengdu, China.

Ecober X., Egusquiza E., Farhat M., Avellan F. and Coussirat M., 2006. “Detection of cavitation in hydraulic turbines”. *Mechanical Systems and Signal Processing*. Vol. 20, p. 983-100.

Hammit F. G., 1979. “Cavitation erosion: the state-of-the-art and predicting capability”. *Applied Mechanics Reviews*. Vol. 32, p. 665-675.

Hazel B., Coté J., Laroche Y. and Mongenot P., 2012. “A Portable, Multiprocess, Track-Based Robot for In Situ Work on Hydropower Equipment”. *Journal of Field Robotics*. Vol. 29, p. 69-101.

Liu, Z-Z., Liu, H-Y and Luo, Z., 2012. “Inverse Kinematics Analysis of 5-DOF Robot Manipulators Based on Virtual Joint Method”. *Applied Mechanics and Materials*. Vol143, p. 265-268.

Motta, J. M. S. T., 2006. “Robot Calibration: Modeling Measurement and Applications”. In *Industrial Robotics: Programming, Simulation and Applications*. Low Kin Huat (Ed.). Croatia: InTech., pp. 107-130.

Motta, J. M. S. T., Llanos, C. H., Carvalho, G. C. and Absi-Alfaro, S. C., 2010a. “A Prototype of a Specialized Robotic System for Repairing Hydraulic Turbine Blades”. In: *1st International Conference on Applied Robotics for the Power Industry (CARPI2010)*, Montreal, Canada.

Motta, J. M. S. T., Carvalho, G. C., Llanos-Quintero, C. H., Vidal-Filho, W. B. and Vasconcelos-Filho, E. P., 2010b. A Specialized Welding Robot for Repairing Hydraulic Turbine Blades”. In Victor J De Negri (Ed). *Symposium Series in Mechatronics*, Vol. 4. Brazil: ABCM. pp.700-709.

Motta, J. M. S. T., Llanos, C. H., Carvalho, G. C., Absi-Alfaro S., Idrobo-Pizo G. and Sampaio, R. C., 2014. “A Specialized Robotic System Prototype for Repairing Surface Profiles of Hydraulic Turbine Blades”. In *3rd International Conference on Applied Robotics for the Power Industry (CARPI2014)*, Foz do Iguassu, Brazil.

Park, J., Kim, J-M., Park, H-H., Kim, J-W., Kang, G-H. and Kim, S-H., 2012. “An Iterative Algorithm for Inverse Kinematics of 5-DOF Manipulator with Offset Wrist”. *World Academy of Science, Engineering and Technology*. Vol. 6, p 144-149.

Parmar R. S., 1997. *Welding processes and technology*. Khanna Publishers, Delhi, p. 808.

Su, D., Calderon, C. A. A., Gan, J. Q. and Hu, H., 2005. “An Analysis of the Inverse Kinematics for a 5-DOF Manipulator”. *International Journal of Automation and Computing.* Vol. 2, p. 114-124.

Xiang, K., Sun, Z., Dai, H., et al., 2010. “CAN-Bus Based Distributed Control System for Hydraulic Turbine Blade Repairing Robot”. In *3rd International Conference on Intelligent Robotics and Applications (ICIRA).* Shanghai, China. Lecture Notes in Artificial Intelligence. 6425: pp 695-704.

8. RESPONSIBILITY NOTICE

The authors are the only responsible for the printed material included in this paper.